NASA B-57B Severe Storms Flight Program

Wenneth D. Painter and Dennis W. Camp

December 1983

NASA
National Aeronautics and
Space Administration

NASA B-57B Severe Storms Flight Program

Wenneth D. Painter and Dennis W. Camp
NASA Ames Research Center, Dryden Flight Research Facility, Edwards, California 93523

NASA B-57B SEVERE STORMS FLIGHT PROGRAM

Weneth D. Painter
NASA Ames Research Center, Dryden Flight Research Facility
Edwards, California   93523

Dennis W. Camp
Atmospheric Sciences Division, Systems Dynamics Laboratory
NASA Marshall Space Flight Center
Huntsville, Alabama   35812

INTRODUCTION

"Takeoff thrust!" shouted the First Officer William Eberhart, as the indicated airspeed of the Eastern Airlines B-727 (Flight 66) decreased from 145 KIAS to 122 KIAS, the aircraft then sank at a high rate toward the approach lights of runway 22L at New York's John F. Kennedy International Airport. First Officer Eberhart's last command was a reflexive attempt to get maximum performance from the aircraft, but it was too little too late. A severe downburst wind shear, flowing out of a thunderstorm cell on the approach path, already had robbed the B-727 of too much energy. Less than 2 sec later, Flight 66 hit the nonfrangible approach lights and began to break up. Of the 124 persons aboard, 113 died of injuries sustained in the crash and ensuing fire. The date was June 24, 1975 (ref. 1).

On August 7, 1975, less than 2 months later, Continental Airlines Flight 427, another B-727, crashed shortly after takeoff from Stapleton Airport in Denver, Colorado. It seemed a miracle that the crash resulted in only 10 serious injuries and no fatalities. Again, the crash was a result of low-level wind shear. More recently, wind shear was listed as the probable cause of the Pan American Flight 759 crash at New Orleans International Airport on July 9, 1982.

Unexpected, low-level wind shear still haunts the skies around virtually all airports. Forcasting wind shear, however, remains an imperfect science at best. Downburst shears, the cold cascades of air that pour from the undersides of some thunderstorm cells, usually are very localized, last only a few minutes, and are spawned by convection weather with complex dynamics.

Severe wind shear and microbursts at low altitudes pose an extreme hazard to aircraft, especially larger, swept wing jet transports, during final approach and takeoff. In these conditions, with the aircraft operating near stall speeds, a

significant change in wind velocity can easily result in a dangerous rate of descent.

The meteorological phenomena producing low-level wind shear and microburst are primarily thunderstorms, thunderstorm gust fronts, and fast-moving frontal zones. In almost all cases microbursts are detected, if detected at all, after the fact. An aircraft approach into a wind shear condition is shown in figure 1.

Low-level wind shear is defined as wind shear occuring between the surface and 1,500 ft (490 m) above ground level. Wind shear is any change in wind speed or direction through a shallow layer of the atmosphere. A microburst is defined as a downdraft and radial outflow near the surface having a horizontal extent less than 2.5 miles (4 km). Measured horizontal wind speeds in a microburst are 20 to 100 mph, lasting between 2 and 8 min. The low-level wind shear associated with the microburst has been implicated as a cause of several major accidents, primarily because the microburst, when penetrated in any direction, whether on takeoff or landing, produces a severe loss of performance in transport aircraft.

Figure 1 is a conceptual drawing of a microburst wind shear which illustrates its effect on an aircraft whether on takeoff or landing. The aircraft will first encounter a rapidly increasing headwind (performance increasing), then encounter the remnants of the microburst (performance decreasing), and finally a rapidly increasing tailwind (performance decreasing). The effect will be similar on departure. To understand just how these phenomena form, and what can be done to detect and avoid them, the National Center for Atmospheric Research (NCAR) and the University of Chicago developed a program to investigate the wind-shear phenomenon. The National Oceanic and Atmospheric Administration (NOAA), the National Aeronautics and Space Administration (NASA), the National Science Foundation (NSF), and the Federal Aviation Administration (FAA) are sponsoring the effort, as well as participating in the overall program. The NASA B-57B airplane was a vital part of this study.

The results of overall meteorology hazards research, involving turbulence, lightning, wind shear, heavy-rain effect, and airborne Doppler radar, is expected to provide information about the characteristics of atmospheric hazards for use in systems design and protection, flight-training simulators, and air-crew procedures.

The spanwise gust gradient program of NASA is an outgrowth of the efforts of several persons who are concerned with improving aviation safety and efficiency. These efforts have been manifested most directly at NASA's Office

2

of Aeronautics and Space Technology (OAST) retreats and at
the Annual Workshops on Meterological and Environmental
Inputs to Aviation Systems. With the selection of the B-57B
aircraft as the data-collection platform, the program moved
from the discussion stage to an active program. The reason
for selecting the B-57B is that it is structurally a very
rigid aircraft, that is, the natural vibrations inherent in
the aircraft are much higher than the wind frequencies of
concern for the gust gradient program.

B-57B AIRCRAFT

The B-57B aircraft used to obtain data in low-level wind
shear and microburst conditions is pictured in figure 2; its
dimensions and other particulars are given in figure 3.
The B-57B was equipped with three booms, one located at the
nose of the fuselage and one at each wing tip. These booms
provided the three components of wind velocity. The air-
plane contained 58 channels of data, which are summarized in
table 1.

DATA-COLLECTION SITES

Figure 4 shows the locations where data have been collec-
ted and locations where data collection is planned in the
future. To date, data have been collected in the areas of
Edwards AFB, California; Denver, Colorado; the Marshall
Space Flight Center, Huntsville, Alabama; and Oklahoma City,
Oklahoma.

The Edwards AFB data collection has been in conditions of
strong wind shear and profile-stability effects from moun-
tain waves and desert heating. Data collection in the
Denver area was in conjunction with the Joint Airport
Weather Studies (JAWS) project in July, 1982 (refs. 2, 3).
The Denver area provided the most data to date. Eleven
data-collection flights (table 2) were conducted during the
3 weeks of flying out of Denver. This site was selected for
many reasons, the most important of which is that the Denver
area has one of the highest thunderstorm rates of any area
in the United States. Another reason for choosing Denver
was the availability of support facilities there. These
facilities included for example radar, weather tower, rawin-
sondes, and meterological networks. Along with availability
of facilities, it was also desirable that the output of the
facilities be readily available and in a format easily
usable. It is believed that these requirements were met at
the data collection sites.

3

During the JAWS project, May 15, 1982 to August 13, 1982, about 70 microbursts were recorded in good dual Doppler-radar coverage where data were collected. Additional data sets were collected in downbursts (large-scale microbursts) gust fronts, mesocyclones, tornadoes, funnel clouds, hail storms, and flash floods (see table 3). In addition, many excellent data sets were gathered on nowcasting utilization of meteorological Doppler radar in a next-generation rada r (NEXRAD) mode. The JAWS project has emerged as one of the most successful research field progra ms that has been conducted in the field of aviation meteorology.

The B-57B Severe Storms Airplane data were digitally recorded on a data recorder carried in the B-57B. A single tape, holding as much as 1.5 hr of flight data, was then shipped to NASA Langley Research Center (LaRC) at Hampton, Virginia, for conversion to engineering units (m/sec, rad/sec, etc). The resulting data were then transmitted to Marshall Space Flight Center (MSFC) at Huntsville, Alabama, and the University of Tennessee Space Institute at Tullahoma, Tennessee, for analysis.

DATA ANALYSIS

The program is summarized in figure 5, which shows the purpose of the effort: namely, to make measurements of wind variations over the span of an airfoil. A schedule of events, from program development to completion of analysis, is also shown. In the upper right of the figure, the need for the effort is illustrated, as well as some key features. The bottom half of the figure shows desired flight track for data collection relative to a storm, the flight-plan profile and a picture of the aircraft.

Figure 6 is a simplified sketch illustrating the need for the Gust Gradient Program as well as its objective. Houbolt (ref. 4) best stated the objective:

> The left side of [figure 6] depicts the assumption commonly used in power spectral treatments of gust encounter; that is, the turbulence is considered random in flight direction but uniform in the spanwise direction. The right side of the figure depicts the more realistic situation wherein the turbulence is considered to be random in both the flight and spanwise directions.

As a result of the statements and figure by Houbolt, it is easy to see that the assumption that an aircraft is completely embedded in a single wind field (gust) is not

really valid, especially when considering wide-body air-
craft. Thus, the objective is to obtain gust data for air-
craft design and also for use in flight-crew training in
simulators. Specifically, the program is to obtain data on
turbulence patchiness and spanwise gust gradients in a
representative variety of atmospheric conditions from several
sites (see fig. 4) for aircraft design purposes and safety
of operations. Emphasis will be on developing models appli-
cable top approach and departure flight paths under condi-
tions of strong wind shear and profile-stability effects.
It is expected that during the course of this program the
B-57B will be used to obtain approximately 60 hours of
flight data during an 18-month period.

The various sites selected (fig. 4) where gust-gradient
data were and are to be collected give a cross section of
topographical features of the United States: coastal,
piedmont, mountainous, and desert areas. In selecting these
sites, it was believed a variety of weather conditions would
be observed having features influenced by the topography.

After the aircraft and instrumentation were checked out
at the Langley Research Center in Virginia, the first data
for analysis were collected in the Denver area during the
JAWS Project (refs. 2,3). The second, third, and fourth
sets of data for analysis were collected in late 1982 and
early 1983 at the Dryden Flight Research Facility, Edwards,
California; May, 1983 at the Marshall Space Flight Center,
Huntsville, Alabama and in the Oklahoma City area.

The data to be presented here were obtained during the
JAWS Project during July 1982. Eleven data collection
flights (table 2) were conducted during this 1-month period.
Table 4 lists the specific data to be presented in this
paper. The data were obtained in the afternoon of July 15,
1982. Data from run 10 of flight 7 is the particular data
set to be discussed. This data run, as can be seen in
figure 7, was made in the vicinity of Longmont, Colorado,
about 25 miles north of Denver. Data for five runs of
flight 7 are plotted in figure 8, in which the horizonal
wind vectors are depicted. The length of each arrow is pro-
portional to the length of the 4-sec average wind (160 data
points). The aircraft heading is from the corner or side of
the box to which the end of the track is closest. In other
words, the heading is always toward the center of the box.
True north is toward the top of the figure. As an example,
in flight 7, run 10, the heading was northeast. Some of the
plots show alternating regions of convergence and divergence.
The wave-like patterns are noticeable in runs 11-140. These
plots are useful for indicating possible outflow features,
and for understanding the general meteorological setting of
the turbulence data.

The most likely penetration of a microburst occurred during flight 7, run 10. The encounter occurred at an altitude of 400 m (1,300 ft)/ACL. The encounter altitude was too high to be in the surface outflow region. The feature appears at about 75 sec into the run. Figure 8 (run 10), shows the wind vector changing from headwind to tailwind over a distance of about 2 km. Figure 9 shows the center boom airspeed trace for run 10. The airspeed plot indicates two possible outflow features occurring at 50 sec and 80 sec into the run. Figure 10 shows the longitudinal, lateral, and vertical turbulent velocities for run 10. The lower part of the figure shows the differences of the three velocity components from wing tip to wing tip. The vertical velocity component shown in figure 10 indicates that the feature at 50 sec is not associated with a downdraft. The second feature is associated with a strong downdraft in excess of 10 m/sec (20 knots). The only negative microburst evidence is that the temperature drop across the apparent microburst front is only of the order of 1°C. An interesting aspect of the turbulent structure is shown at the lower part of figure 10: if the uniformly modulated model of turbulence (ref. 5) is invoked for the velocity differences, then

$$V(t) = \sigma_{\Delta V}(t)\, Z(t)$$

where $Z(t)$ is a stochastic process with unit standard deviation and zero mean value, and a $\sigma_{\Delta V}(t)$ is the time-varying standard deviation with a much slower variation with time than $Z(t)$. Based on the velocity-difference data shown in figure 10 and in Camp et al. (ref. 6), this model is quite reasonable. The interesting feature of the downdraft structure is that the velocity-difference, time-varying standard deviation, $\sigma_{\Delta V}$, shows a marked decrease for all three velocity components within the downdraft. The decrease of $\sigma_{\Delta V}$ within the downdraft raises three possibilities; either the three turbulent intensities decrease within the downdraft, or the turbulent length scales increase, or a combination of both occur. From the lower half of figure 10 some decrease in the turbulent intensity is apparent in the longitudinal component, but it is not so apparent in the other two components. If the downdraft is modeled as a circular jet, observations by Wygnanski and Fiedler (ref. 7) show that the turbulent intensity is highest at the center of the jet. The reason for the discrepancy is unknown; however, in the vicinity of storms (but outside of clouds) inflowing air is frequently observed to be smooth.

The turbulent velocities shown in figure 10 reveal some large scale trends. In the difference data, the trends are naturally filtered out. Large-scale phenomena influence all the probes on the B-57B simultaneously and differencing

removes these effects. The large-scale structures cause probability-density functions to have a round, jagged appearance, as shown in figure 11. Indeed, for the u and v components, the density function has a general bimodal appearance. The vertical component is unimodal, but has a rough appearance. The right side of figure 11 shows the density function for wing-tip-to-wing-tip difference data. As expected, the differences have a much smoother appearance because the large-scale structures are filtered out by the differencing process. These curves for flight 7, run 10 are fairly typical for all runs analyzed so far.

The probability-density functions for the difference data show a consistent non-Gaussian behavior. Although skewness is nearly zero, the kurtosis (peakiness) of the data is consistently higher than the Gaussian value of three. The idea that atmospheric turbulence is non-Gaussian is not new, as indicated by Dutton (ref. 8), and Batchelor (ref. 9). Frenkiel and Klebanoff (ref. 10) even show that the wind-tunnel turbulence behind grids is non-Gaussian. Although individual velocity components show approximately Gaussian (marginal) distributions, joint distributions of more than one velocity are non-Gaussian.

The question of whether the distribution of the velocity differences is Gaussian can be important. For example, if an aircraft structure is designed to withstand a certain wing-loading level, which a Gaussian model says will be encountered only once in 1,000 hrs of flying, the structure may fail prematurely because the Gaussian model will underestimate the frequency of occurrence of large gust differences. A Gaussian model of excessive gust differences across an airfoil is highly unrealistic, and the frequency of occurrence of values out on the wings of the probability density function can be significantly underestimated.

Figure 12 is a plot of kurtosis versus skewness of the velocity difference data for 10 severe turbulence runs, five from flight 6 and five from flight 7. Each data point corresponds to one run and one component. Although the skewness values are nearly zero, the kurtosis values for each velocity-difference component are never less than 3.8 for any of the 10 runs. The average value kurtosis is about 5 for the u and v components, and 6 for the w component.

The form that a difference model should take can be estimated using the Pearson family of probability curves, as shown by Elderton and Johnson (ref. 11). Pearson based his family of curves on solutions of a differential equation, and divided shewness-kurtosis space into several regions. In each region a different probability distribution was thought to best fit the data. Each data point falls within the Pearson type-IV region but is very close to the

skewness = 0 Pearson VII line. The question arises as to whether a Pearson type-VII or a Pearson type-IV curve should be used to model the velocity differences. The answer hinges on whether the real skewness is zero. The small observed deviations from zero may be statistical errors of sampling. Is there any good reason to expect the skewness to be nonzero? For isotropic turbulence, the skewness for the u and w velocity differences is zero, but for v may possibly be nonzero. In any event, the observed values are very nearly zero, and for that reason, the Pearson type-VII distribution will probably be suitable for most purposes. The Pearson type-VII distribution is closely ralated to (Student's t) distribution.

SUMMARY

Plots of winds encountered in-flight were presented for a severe turbulence case from JAWS flight 7. This set of data has been analyzed in some detail. During the flight, the B-57B showed a 30-knot (15-m/sec) increase in airspeed over a distance of about 426 ft (130 m) and then a more gradual decrease of 40 to 50 knots (20 to 25 m/sec) over a distance of about 3.2 miles (5.1 m). This suspected outflow feature was associated with downdraft in excess of 20 knots (10 m/sec). The horizontal wind direction changed almost 180° during the pass through the feature. Somewhat suprisingly, the intensity of velocity differences decreased for all three components within the downdraft.

Calculated probability-density functions for u,v, and w showed a jagged character, and Δu, Δv, and Δw showed a much smoother, unimodal behavior. Distributions for Δu, Δv, and Δw were distinctly non-Gaussian. Based on skewness, and kurtosis values, the data could probably best be modeled by a Pearson type VII (Student's t) distribution. The non-Gaussian behavior was not unexpected, but was important because Gaussian models could significantly underestimate the frequency of occurrence of extreme values of velocity differences.

Figures 11 and 12 illustrate the kind of information desired from the B-57B Gust Gradient Program: What type of wind distribution should be used in the design of future aircraft, and how should the wind variability be used in flight simulation for air-crew training? As more of the gust-gradient data are analyzed, it is expected that the answer to these questions will be clearer.

8

REFERENCES

1. Aircraft Accident Report; Eastern Airlines, Inc., Boeing 727-225, N8845E, National Transportation Safety Board, NTSB-AAR-76-8 June 24, 1975.

2. McCarthy, John; Wilson, J.; and Fujita, T.: The Joint Airport Weather Studies Project (JAWS) AIAA-82-0017. Presented at AIAA 20th Aerospace Sciences Meeting, Orlando, Fla., Jan. 1982.

3. McCarthy, John: The Joint Airport Weather Studies Project. NASA CP-2192, pp. 91-95.

4. Houbolt, John C.: Effect of Spanwise Gust Variations. NASA CP-2104, 1979, pp. 72-79.

5. Mark, W. D.; and Fischer, R. W.: Investigation of the Effects of Nonhomogeneous (or Nonstationary) Behavior on the Spectra of Atmospheric Turbulence. NASA CR-2745, 1976.

6. Camp, Dennis; Campbell, Warren; Frost, W.; Murrow, H.; and Painter, W.: NASA's B-57B Gust Gradient Program AIAA-83-0208. Presented at AIAA 21st Aerospace Sciences Meeting, Reno, Nev., Jan. 1983.

7. Wygnanski, I.; and Fiedler, H.: Some Measurements in the Self-Preserving Jet. J. Fluid Mech., vol. 38, 1969, pp. 566-612.

8. Dutton, John A.: Effects of Turbulence on Aeronautical Systems. Progress in Aerospace Sciences, vol. 11, Pergamon Press, London, 1970.

9. Batchelor, B. K.: The Theory of Homogeneous Turbulence. Cambridge University Press, Cambridge, 1960.

10. Frenkiel, F. N.; and Klebanoff, P. S.: Higher Order Correlations in a Turbulent Fluid. Phys. Fluids, vol. 10, 1967, pp. 507-520.

11. Elderton, W. D.; and Johnson, N. L.: Systems of Frequency Curves. Cambridge University Press, Aberdeen, 1969.

Table 1. B-57B data channels.

Channel	Quantity	Range	Resolution
1	Time, sec	---	0.001 sec
2	Roll velocity, rad/sec	1 rad/sec	0.002
3	Normal acceleration at the cg, g	+5, -3g	0.004
4	Pitch velocity, rad/sec	1 rad/sec	0.002
5	Pitch attitude, rad	15°	0.03
6	Roll attitude, rad	15°	0.03
7	Heading relative to true north, deg	0-360°	0.14 arc-sec
8	Heading relative to time zero heading, deg	0-360°	0.14 arc-sec
9	Heading relative to true north, differential range, deg	0-360°	0.14 arc-sec
10	Differential range heading relative to time zero heading, deg	---	0.14 arc-sec
11	Normal acceleration at left wingtip, g	+5, -3g	0.004
12	Normal acceleration at right wingtip, g	+5, -3g	0.004
13	X acceleration at the cg, g	1g	0.002
14	Y acceleration at the cg, g	1g	0.002
15	Angle of attack at the nose boom, rad	15°	0.03
16	Angle of sideslip at the nose boom, rad	15°	0.03
17	Temperature of the INS pallet, °F	---	0.1
18	Temperature of the instrument pallet, °F	---	0.1
19	Z acceleration INS, g	±1g	0.004
20	Angle of attack at right boom, rad	±15°	0.03
21	Sideslip angle at right boom, rad	±15°	0.03
22	Angle of attack at left boom, rad	±15°	0.03

Table 1. Continued.

Channel	Quantity	Range	Resolution
23	Sideslip angle at left boom, rad	±15°	0.03
24	Yaw rate, rad/sec	1 rad/sec	0.002
25	Total temperature, °C	---	0.1
26	Impact pressure at the left boom, psid	0-3 psi	0.0004
27	Impact pressure at the center boom, psid	0-3 psi	0.0004
28	Impact pressure at the right boom, psid	0-3 psi	0.0004
29	Static pressure at the center boom, psia	0-15 psia	0.0004
30	Temperature from IR radiometer, °C	---	---
31	Large distance (word overflow)	---	---
32	Bearing to destination, deg	0-360°	0.14 arc-sec
33	Longitude, deg	±90°	0.14 arc-sec
34	Latitude, deg	±180°	0.14 arc-sec
35	Track angle, deg	0-360°	0.14 arc-sec
36	Heading, rad	0-360°	0.14 arc-sec
37	Airplane east-west inertial velocity, m/sec	±1200 m/sec	0.0003 m/sec
38	Airplane north-south inertial velocity, m/sec	±1200 m/sec	0.0003 m/sec
39	Altitude, km	---	---
40	Computed free-air temperature, °C	±35-65°C	0.1
41	East-west windspeed, knots	---	---
42	North-south windspeed, knots	---	---
43	Windspeed, knots	---	---
44	Wind direction, deg	---	---
45	Airspeed R, m/sec	1200 m/sec	0.0003 m/sec
46	Airspeed C, m/sec	1200 m/sec	0.0003 m/sec
47	Airspeed L, m/sec	1200 m/sec	0.0003 m/sec
48	Altitude change from start of run, m	---	---
49	Inertial displacement, m	---	---

Table 1. Concluded.

Channel	Quantity	Range	Resolution
50	UG R, m/sec	---	0.3 m/sec
51	UG C, m/sec	---	0.3 m/sec
52	UG L, m/sec	---	0.3 m/sec
53	VG R, m/sec	---	0.3 m/sec
54	VG C, m/sec	---	0.3 m/sec
55	VG L, m/sec	---	0.3 m/sec
56	WG R, m/sec	---	0.3 m/sec
57	WG C, m/sec	---	0.3 m/sec
58	WG L m/sec	---	0.3 m/sec

Table 2. Gust gradient flights during JAWS 1982.

Flights	Date	Starts	Ends	Comments
1	7/7	15:41:38	15:59:39	Landmark familarization flight
2	7/8	15:49:11	16:40:35	Light to Moderate Turbulence
3	7/9	13:17:10	15:42:34	Light to Moderate Turbulence with Data Correlation with JAWS 02 and 30
4	7/11	14:46:07	17:02:44	Moderate Turbulence and Lighting
5	7/13	15:20:18	16:44:56	ILS Approaches to Stapleton in Light Turbulence
6	7/14	13:41:13	15:55:21	Severe Turbulence and Outflows Visible of Radar
7	7/15	14:08:13	16:26:20	Outflows, Severe Turbulence, and ILS Approches
8	7/17	15:49:35	17:17:56	Rain with Light to Moderate Turbulence
9	7/20	15:59:30	18:35:52	Light to Moderate Turbulelnce with Some ILS Approaches
10	7/21	16:05:05	18:04:40	Good Downburst with Moderate to Severe Turbulence
11	7/22	13:36:09	15:24:45	Light and Moderate Turbulence

Table 3. JAWS weather statistics.

Event	Number of days
Research days	91
Storm days	78
MIcroburst days	33
Number of Microbursts	70*
Gust front days	41
Mesocyclone or tornado days	22
Hail days (observed by COSIG or at a radar)	12
Days of insignificant or no weather	13

*Approximately 70 microbursts were identified by Doppler radar.

Table 4. Processed B-57B JAWS Flights, flight 7.

Run	Start time	Stop time	Duration, sec
10	15:14:55	15:17:30	155
11	15:18:42	15:21:07	145
12	15:22:50	15:25:10	140
13	15:27:20	15:29:28	151
14	15:31:20	15:33:43	131
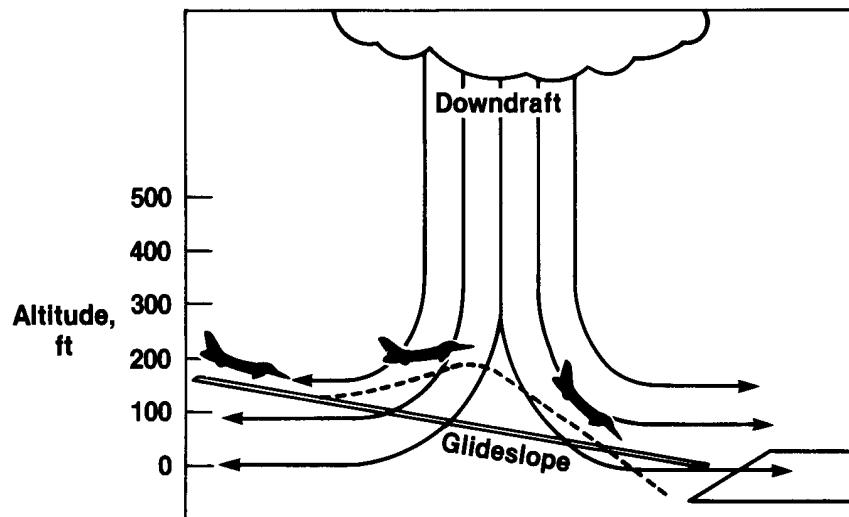
Fig. 1. *Schematic diagram (not to scale) of an aircraft landing in a microburst. The aircraft first encounters rapidly increasing headwinds (performance increasing), then encounters the remnants of the downdraft (performance decreasing), and finally a rapidly increasing tailwind (performance decreasing). The effect would be similar on departure.*
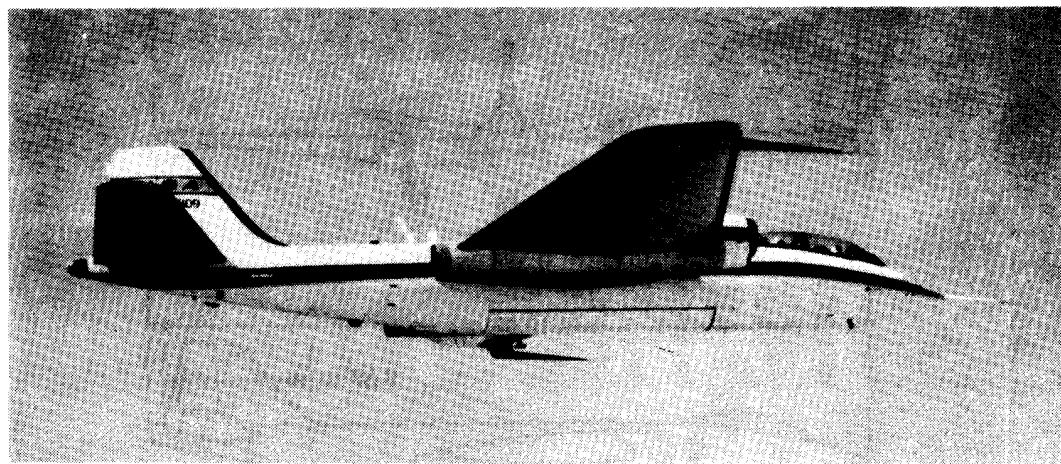
Fig. 2. *B-57B aircraft in flight.*
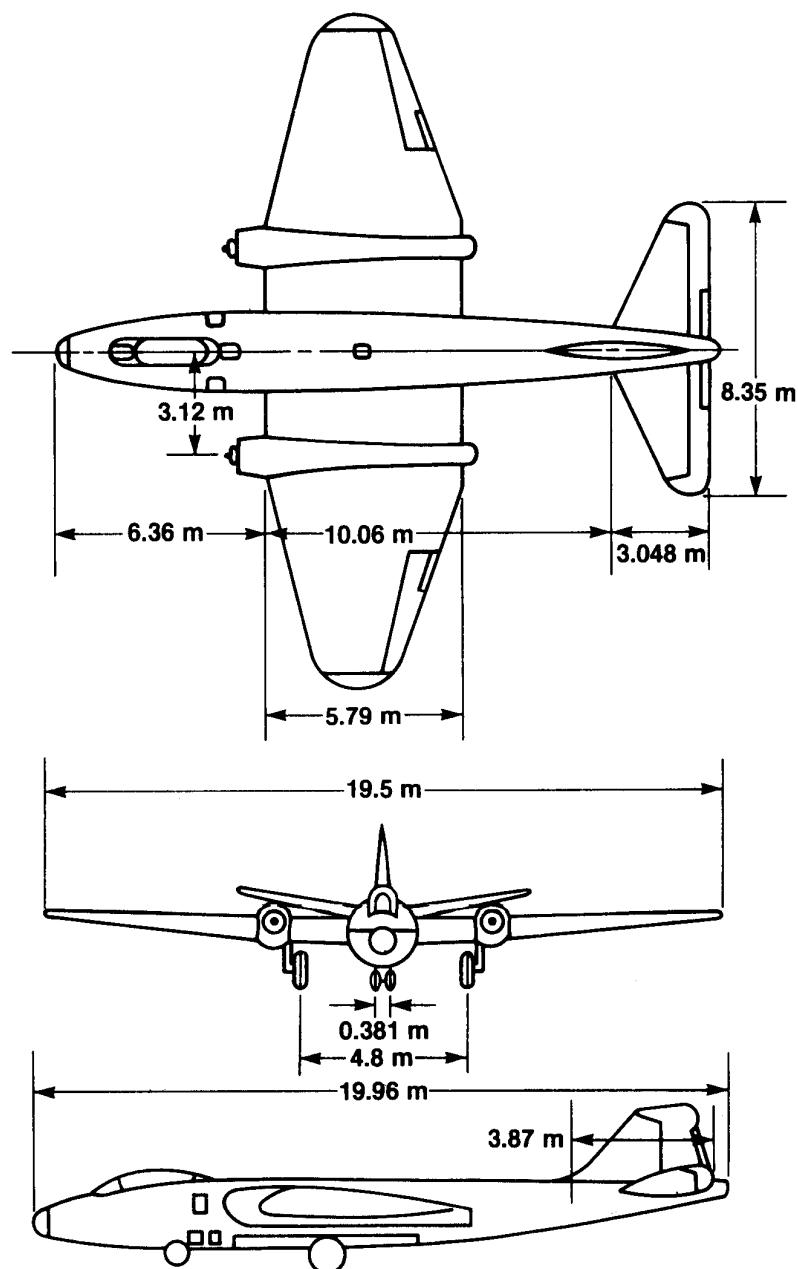
Fig. 3. B-57B aircraft particulars.
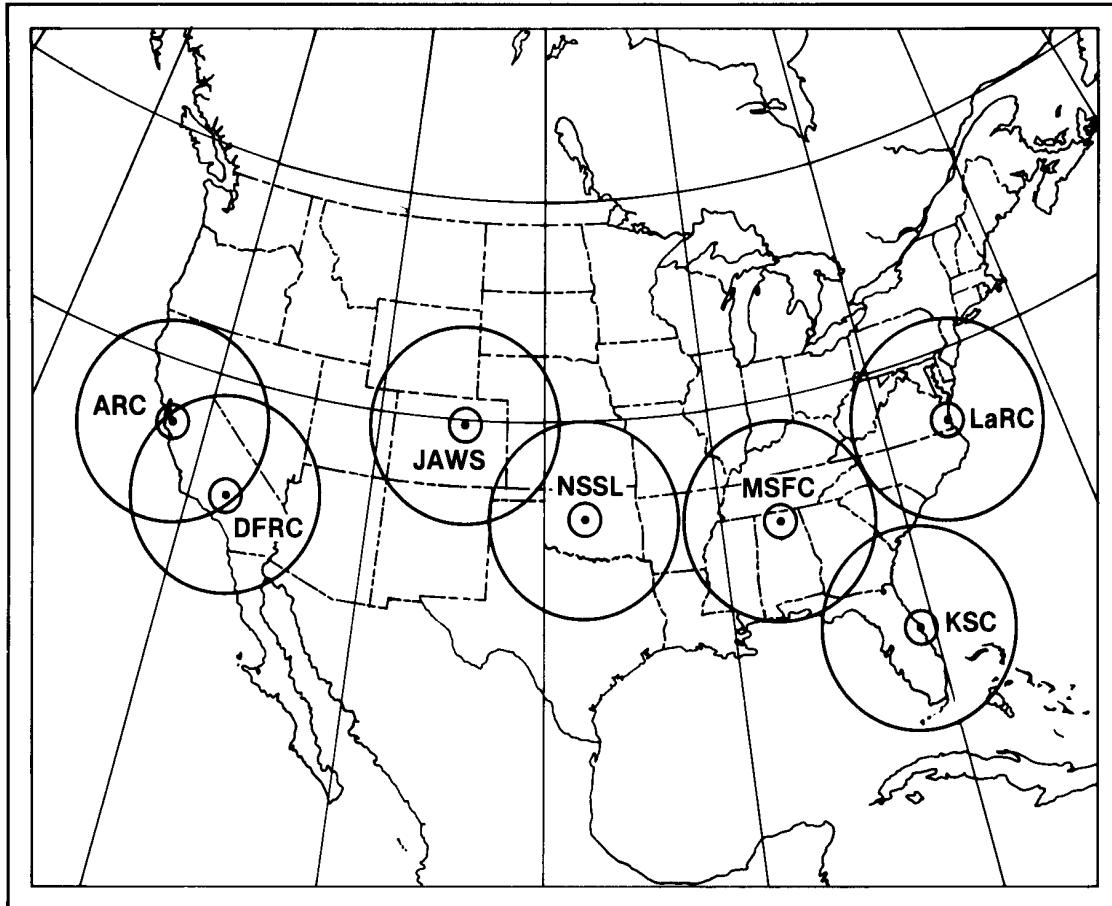
Fig. 4. B-57B coverage: radii = 62 and 310 miles (100 and 500 km).

Measurement of wind variation over span of an airfoil

- Program development 1981
- Measurement tests 1982-83
- Data analysis 1982-84
  Design criteria
  Simulation studies
  Flight crew training

Uniform

Nonuniform

Vertical force

Roll
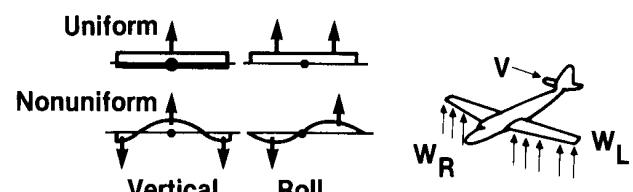
Random gusts assumed to be composed of sinusoidal gusts

V

W_R W_L

Three of the key features of spatial or spanwise gust variations

Cycle 1

Cycle 2

x-Record data

Runway

Storm cell

Cycle 3

Cycle 4

Cycle 1

3°

3°

Cycle 2

Runway
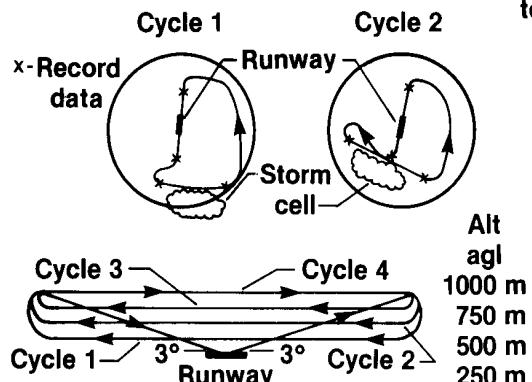
Alt agl
1000 m
750 m
500 m
250 m

Flight plan profile

Flight path for thunderstorm case
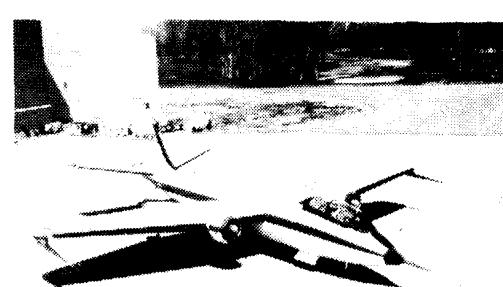
Fig. 5. NASA's B-57B gust-gradient program.
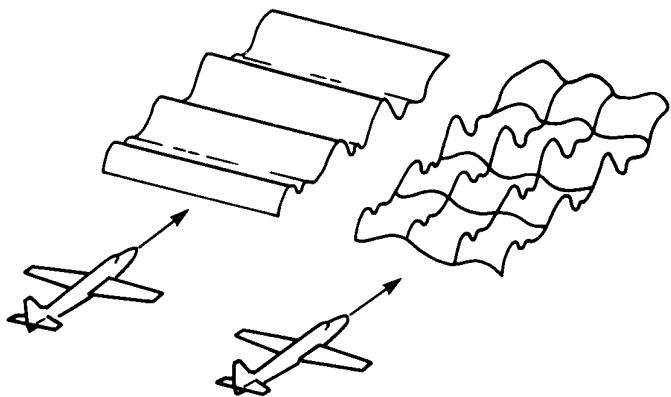
Fig. 6. Assumption of turbulence
models.
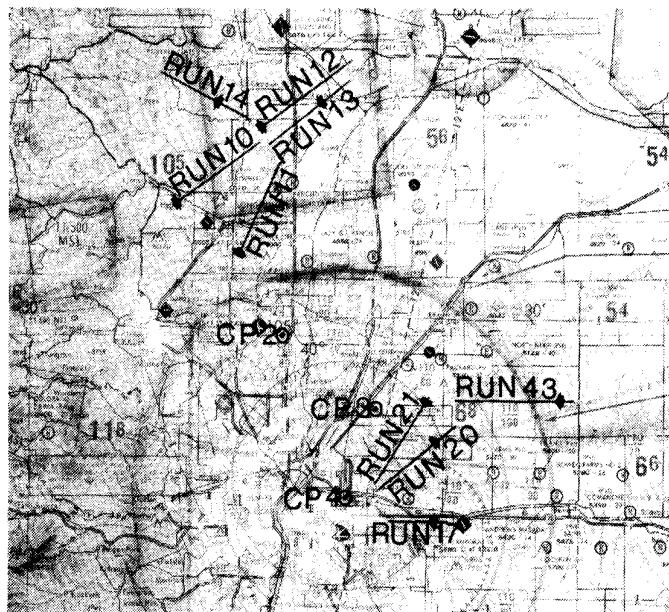
Fig. 7. Ground tracks for JAWS
Flight 6 (runs 17, 20, 21, 43)
and flight 7 (runs 10-14),
July 14-15, 1982.

Run 10

Run 11

Run 12

5 m/sec ⟶

The box is
22.5 km square

Run 13

Run 14

N
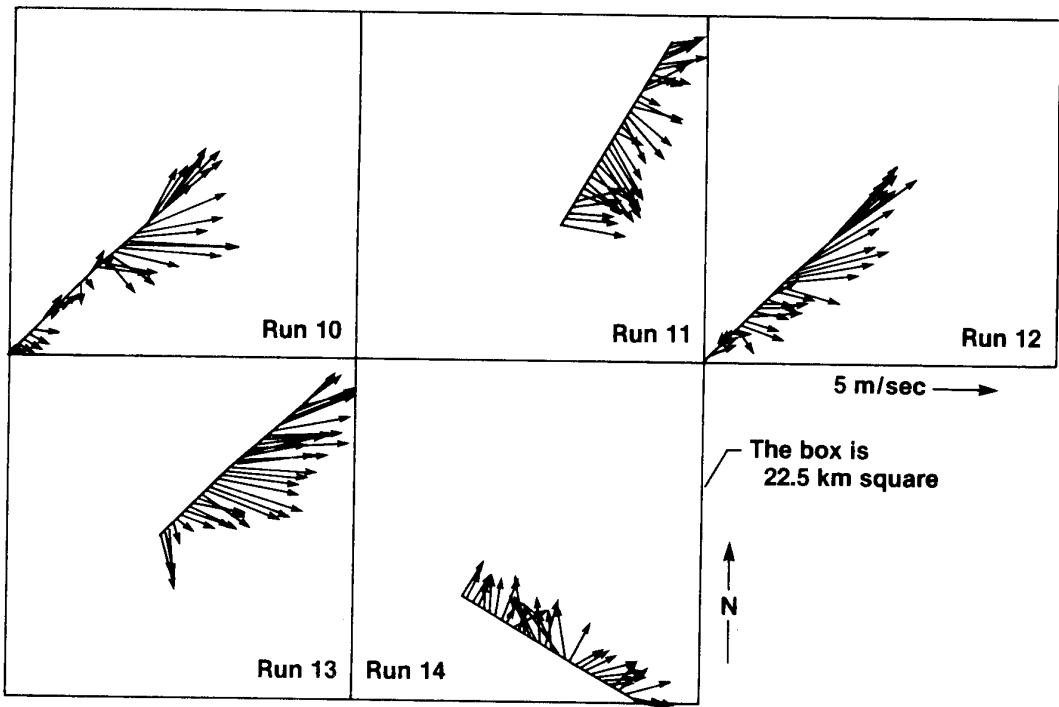
Fig. 8. Horizontal winds encountered by the B-57B during
JAWS flight 7.

Airspeed,
m/sec

150

100

50

0   50   100   150
Time, sec
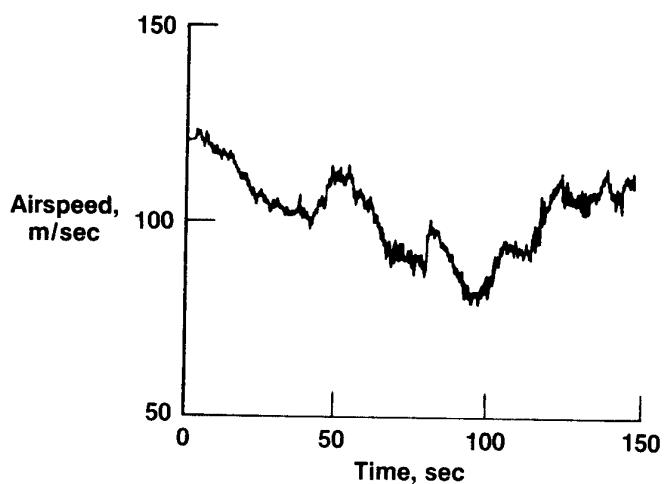
Fig. 9. B-57B airspeed for JAWS
flight 7, run 10.

19
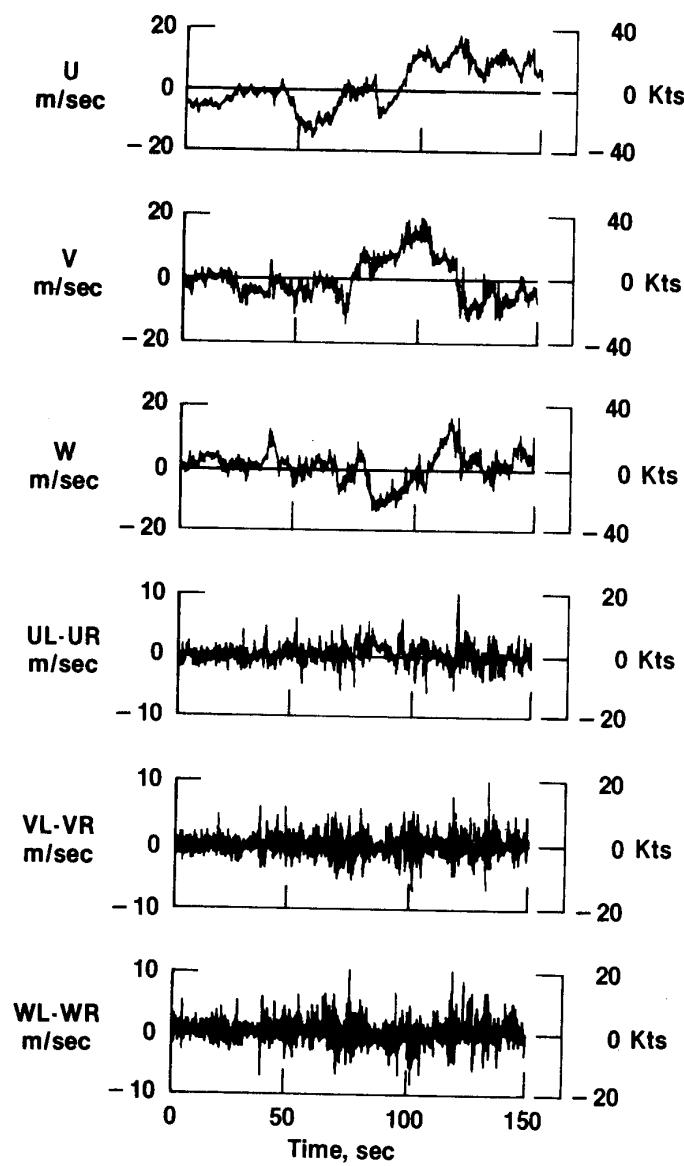
Fig. 10. Gusts and wing-tip-to-wing-tip gust differences for JAWS flight 7, run 10.
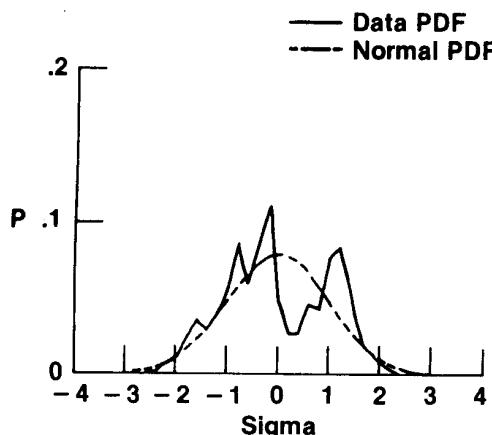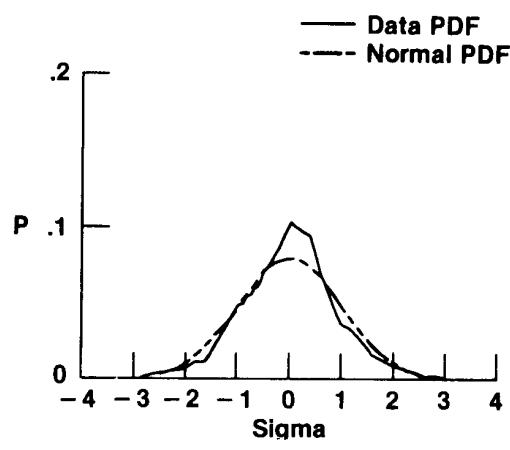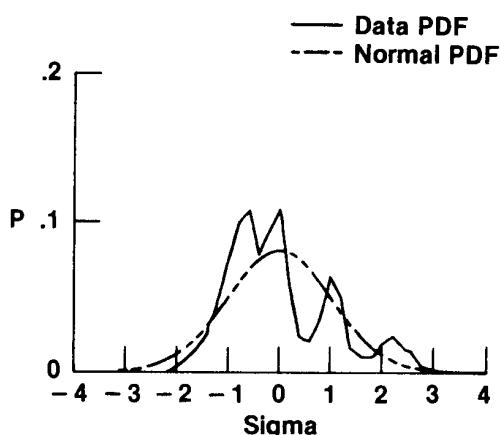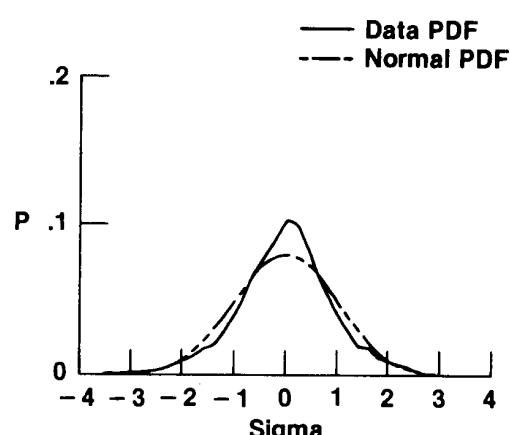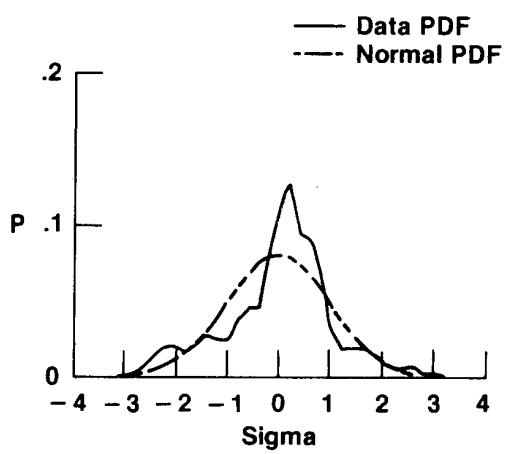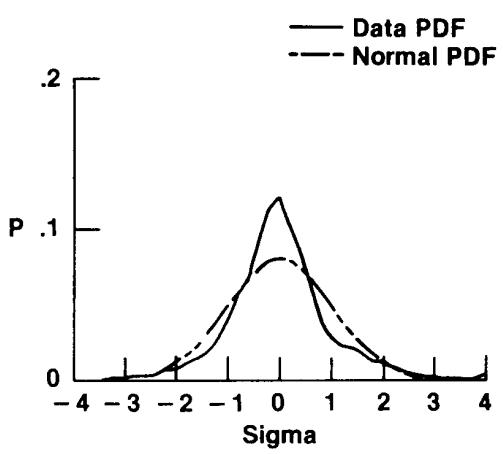
*Fig. 11.* *Probability-density functions for JAWS flight 7, run 10.*
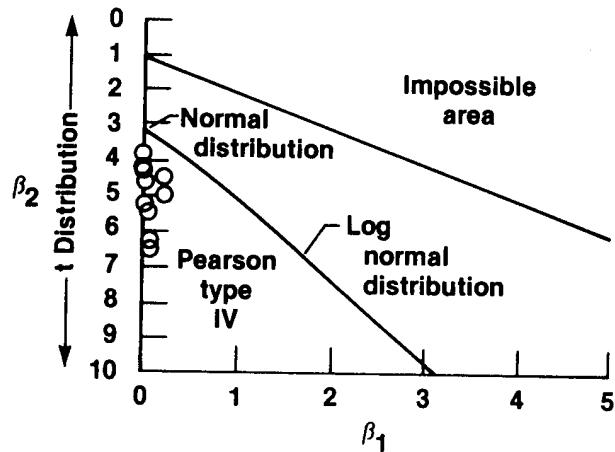
(a)   u component.
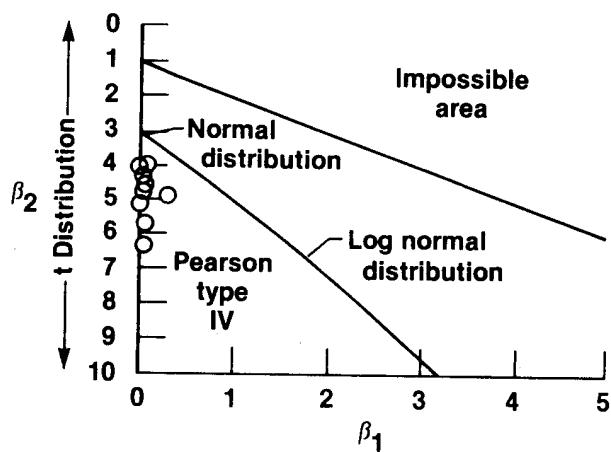
(b)   v component.
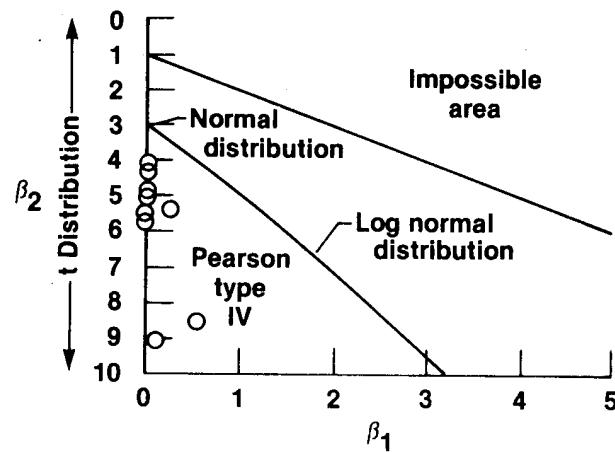
(c)   w component.

Fig. 12.   Kurtosis-skewness plots of velocity differences ($\Delta Y = 19.5$ m) for severe turbulence runs on JAWS flights 6 and 7.

1. Report No. NASA TM-84921	2. Government Accession No.	3. Recipient's Catalog No.
4. Title and Subtitle NASA B-57B Severe Storms Flight Program		5. Report Date December 1983
		6. Performing Organization Code H-1196
7. Author(s) Weneth D. Painter and Dennis W. Camp		8. Performing Organization Report No.
9. Performing Organization Name and Address NASA Ames Research Center Dryden Flight Research Facility P.O. Box 273 Edwards, CA 93523		10. Work Unit No.
		11. Contract or Grant No.
12. Sponsoring Agency Name and Address National Aeronautics and Space Administration Washington D.C. 20546		13. Type of Report and Period Covered Technical Memorandum
		14. Sponsoring Agency Code RTOP 505-45-01

15. Supplementary Notes

16. Abstract

The objective of the B-57B Severe Storms Flight Program is to gather data to characterize atmosphere anomalies such as wind shear, turbulence, and microbursts at altitudes up to 1000 feet (300 meters). These data will be used to enhance our knowledge of atmospheric processes, to improve aviation safety, to develop systems technology and piloting technique for avoiding hazards and to increase the understanding of the causes of related aircraft accidents.

The NASA Dryden Flight Research Facility B-57B aircraft has participated in several severe storms data collection programs such as the Joint Airport Weather Studies (JAWS) located in Denver, Colorado area, Operation Rough Rider located in the Norman, Oklahoma area with the National Severe Storms Laboratory, and Mountain and desert turbulence in the Edwards Air Force Base, California area.

Flight data will be presented from flights which encountered the wind shear, turbulence and microburst anomalies. These flight results will be discussed and some conclusions will be made relating to these atmospheric anomalies.

17. Key Words (Suggested by Author(s)) Severe storms Wind shear Microbursts Turbulence Aviation safety	18. Distribution Statement Unclassified - Unlimited STAR category 03

19. Security Classif. (of this report) Unclassified	20. Security Classif. (of this page) Unclassified	21. No. of Pages 25	22. Price* A02